European Review for Medical and Pharmacological Sciences 2020; 24: 12306-12314

MiR-204 reduces apoptosis in rats with myocardial infarction by targeting SIRT1/p53 signaling pathway

L.-Z. WANG[1], J.-N. XI[1], T.-J. LIU[1], Z.-Y. ZHANG[1], P. ZHANG[1]

Department of Cardiac, Beijing Rehabilitation Hospital, Capital Medical University, Beijing, China

Abstract. – OBJECTIVE: The aim of this study was to investigate the influence of micro ribonucleic acid (miR)-204 on rats with myocardial infarction by targeting the silent information regulator 1 (SIRT1)/p53 signaling pathway.

MATERIALS AND METHODS: A total of 36 Sprague-Dawley rats were randomly divided into three groups, including: sham-operation group (n=12), model group (n=12) and miR-204 mimics group (n=12). The rats in the sham-operation group only underwent thoracotomy, without myocardial infarction injury. Meanwhile, the rats in model group and miR-204 mimics group were utilized to establish the models of myocardial infarction, and then, intervened with normal saline and miR-204 mimics, respectively. The morphology of myocardial tissues was observed via hematoxylin-eosin (HE) staining. Immunofluorescence was performed to detect the expression of Caspase-3. Target genes of miR-204 were analyzed using bioanalysis software. Western blotting (WB) assay was applied to measure the relative protein expression of SIRT1. MiR-204 expression and the messenger RNA (mRNA) expressions of SIRT1 and p53 were measured via quantitative Polymerase Chain Reaction (qPCR). Furthermore, cell apoptosis was determined through terminal deoxynucleotidyl transferase-mediated dUTP nick end labeling (TUNEL) assay.

RESULTS: HE staining showed that the morphology of myocardial tissues was normal in sham-operation group. Severe myocardial tissue injury was visible in model group, and the injury was relieved in miR-204 mimics group when compared with model group. The results manifested that the positive expression of Caspase-3 in cardiac tissues increased remarkably in the model group and miR-204 mimics group in comparison with sham-operation group ($p<0.05$). Meanwhile, it was evidently lower in miR-204 mimics group than model group ($p<0.05$). Based on the analysis via bioanalysis software, SIRT1 was the target gene of miR-204. WB results revealed that the relative protein expression level of SIRT1 was elevated notably in the other two groups compared with the 2sham-operation group ($p<0.05$). However, it was markedly lowered in miR-204 mimics group in contrast with model group ($p<0.05$). QRT-PCR results demonstrated that the model group and miR-204 mimics group exhibited distinctly lower expression of miR-204 but higher mRNA expressions of SIRT1 and p53 than sham-operation group ($p<0.05$). However, miR-204 mimics group exhibited prominently higher expression of miR-204 but lower mRNA expressions of SIRT1 and p53 than model group ($p<0.05$). Finally, the results of TUNEL assay demonstrated that the apoptosis rate increased remarkably in the model group and miR-204 mimics group when compared with sham-operation group ($p<0.05$). However, it decreased notably in miR-204 mimics group in comparison with model group ($p<0.05$).

CONCLUSIONS: MiR-204 reduces the apoptosis level in rats with myocardial infarction via targeted inhibition of the SIRT1/p53 signaling pathway.

Key Words:
Myocardial infarction, MiR-204, SIRT1/p53 signaling pathway, Apoptosis.

Introduction

Myocardial infarction is an ischemic heart disease, in which cardiac function is seriously impaired by ischemic necrosis of myocardial tissues due to inadequate blood supply to the heart. Currently, myocardial infarction is one of the major diseases causing death in the elderly[1-3]. In addition, many young people die from myocardial infarction with the increase of life stress and the acceleration of life rhythm. However, there are no ideal preventive and therapeutic methods for myocardial infarction at present. Therefore, myocardial infarction is still a tough problem facing the clinical workers and medical researchers worldwide.

Corresponding Author: Tiejun Liu, MD, Ph.D; e-mail: urologistliu@hotmail.com

Massive cardiomyocyte apoptosis induced by ischemic and hypoxic changes in myocardial tissues due to inadequate blood supply to the heart is an important pathological process and pathological response during myocardial infarction[4-6]. It is also a vital pathological factor for myocardial tissue repair, ventricular remodeling, and cardiac function recovery. Silent information regulator 1 (SIRT1)/p53 signaling pathway is considered as a crucial signal transduction pathway. Meanwhile, it is also a key signaling pathway regulating inflammation in organisms[7,8]. Activated SIRT1/p53 signaling pathway upregulates cell apoptosis, playing a pivotal role in the pathological mechanism of myocardial infarction.

Micro ribonucleic acid (miR)-204 has been proven to exert important regulatory effects in inflammation, apoptosis, cell proliferation, necrosis, as well as other physiological and pathological processes. It is also able to modulate the activation of signaling pathways and the expression of multiple downstream substances[9,10]. Hence, it can be conjectured that miR-204 may be involved in the pathological mechanism of myocardial infarction by regulating various pathological responses. The aim of this study was to clarify the influence of miR-204 on rats with myocardial infarction by targeting the SIRT1/p53 signaling pathway.

Materials and Methods

Animals and Grouping

A total of 36 Specific Pathogen Free (SPF)-grade laboratory Sprague-Dawley (SD) rats aged 1 month old were purchased from Shanghai SLAC Laboratory Animal Co., Ltd [license No.: SCXK (Shanghai, China) 2014-0003]. All rats were fed adaptively in the Laboratory Animal Center with normal diet and sterile filtered water every day under the conditions of a 12/12 h light/dark cycle, conventional room temperature, and humidity for 7 d before experiments. All the 36 SD rats were divided into three groups, including: sham-operation group (n=12), model group (n=12) and miR-204 mimics group (n=12) using a random number table. This study was approved by the Animal Ethics Committee of Capital Medical University Animal Center.

Reagents

MiR-204 mimics (CST, Danvers, MA, USA), anti-SIRT1 and anti-Caspase-3 primary antibodies and secondary antibodies (Abcam, Cambridge, MA, USA), hematoxylin-eosin (HE) staining, enzyme-linked immunosorbent assay (ELISA) and terminal deoxynucleotidyl transferase-mediated dUTP nick end labeling (TUNEL) assay kits (Beyotime, Shanghai, China), and quantitative Polymerase Chain Reaction (qPCR) kit (Vazyme, Nanjing, China).

Modeling Methods

The rats were first intraperitoneally injected with 3% pentobarbital sodium (5 mL/kg). After successful anesthesia, the rats were fixed on an operation table and connected to an electrocardiogram monitor. Subsequently, the anterior thoracic region was exposed and cut open to expose the heart. Then, the left anterior descending coronary artery was dissected carefully and ligated at 1/2. The color of the left anterior wall of the rat heart was observed closely. When the left anterior wall of the heart turned pale and ischemic changes in myocardium occurred in the electrocardiogram of the monitor, myocardial infarction was successfully induced. About 30 min later, the ligation was removed, blood supply was restored, and the state of rats was observed. Finally, the wound was sutured, and the rats were kept in separate cages.

Intervention Methods

The rats in the sham-operation group only received thoracotomy, without ischemia/reperfusion injury. The rats in model group were infused with normal saline *via* the femoral vein at 5 min before the establishment of myocardial ischemia/reperfusion model. After myocardial ischemia for 30 min, reperfusion was performed, and the wound was sutured. Next, normal saline was infused through the femoral vein every day, followed by sample acquisition after feeding for 7 d. In miR-204 mimics group, the rats were injected with miR-204 mimics (3 μM) from the femoral vein at 30 min before the modeling of myocardial ischemia/reperfusion. Later, the myocardium was subjected to ischemia for 30 min and reperfusion. After that, the wound was sutured, followed by femoral intravenous infusion of miR-204 mimics (3 μM) daily. The rats were fed for 7 d before sample collection.

Sampling Methods

After the rats were anesthetized successfully, cardiac tissues were directly obtained from 6 random rats in each group. Collected tissues were flushed with normal saline, put into Eppendorf (EP, Hamburg, Germany) tubes and stored

at -80°C for later use. As for the remaining 6 rats in each group, the thoracic cavity was cut open to expose the heart. Next, 400 mL of 4% paraformaldehyde was perfused from the left atrial appendage for fixation. Finally, cardiac tissues were taken out and fixed with 4% paraformaldehyde solution.

HE Staining

Paraffin-embedded tissue sections (5 μm-thick) were soaked in xylene solution and graded alcohol for routine deparaffinization. The sections were then stained with hematoxylin dye for 5 min using the HE staining kit. Next, the sections were sequentially soaked in pure water for 10 min, 95% ethanol for 5 s and xylene for 10 s, followed by mounting in neutral balsam.

Immunofluorescence

Paraffin-embedded tissue sections (5 μm-thick) were routinely deparaffinized in xylene solution and graded alcohol in sequence. Subsequently, the sections were immersed in citric acid buffer for antigen retrieval. After reaction with endogenous peroxidase blocker for 10 min, the sections were sealed with goat serum for 20 min after rinsing. Subsequently, anti-Caspase-3 primary antibody (1:200) was added in drops and placed in a refrigerator at 4°C overnight. On the next day, the sections were rinsed and added dropwise with corresponding secondary antibody for 10 min of incubation. After rinsing, the sections reacted with streptavidin-peroxidase solution for 10 min. The color was developed with diaminobenzidine (DAB; Solarbio, Beijing, China), and the nuclei were counterstained with hematoxylin, followed by mounting with neutral balsam.

Western Blotting (WB) Assay

Lysis buffer was added into cryopreserved cardiac tissues for ice bath for 1 h. After centrifugation at 14,000 g in a centrifuge for 10 min, total proteins in tissues were extracted. The concentration of extracted protein was quantified using bicinchoninic acid (BCA) method (Pierce, Rockford, IL, USA). Next, the absorbance and standard curve of the proteins were obtained through a microplate reader, based on which protein concentration in tissues was calculated. Subsequently, total proteins were subjected to denaturation and separated *via* sodium dodecyl sulphate-polyacrylamide gel electrophoresis (SDS-PAGE). The position of the Marker proteins was observed, and the electrophoresis was stopped when the Marker proteins reached the bottom of glass plate in a straight line. Then, the proteins were transferred onto polyvinylidene difluoride (PVDF) membranes (Millipore, Billerica, MA, USA). After sealing with blocking buffer for 1.5 h, the membranes were incubated with anti-SIRT1 primary antibody (1:1000) overnight. On the next day, the membranes were incubated with corresponding secondary antibody (1:1000) at room temperature for 2 h. Immuno-reactive bands were finally developed with chemiluminescent reagent in the dark for 1 min.

Quantitative Reverse Transcription-Polymerase Chain Reaction (QRT-PCR) Assay

Total RNA was first extracted from fresh cardiac tissues. Subsequently, RNA samples were reversely transcribed into complementary deoxyribose nucleic acid (cDNA) using a 20 μL reaction system under the following conditions: reaction at 50°C for 5 min, pre-denaturation at 95°C for 10 min, denaturation at 95°C for 10 s and annealing at 50°C for 30 s for 45 cycles. Relative expression of relevant messenger RNA (mRNA) was calculated, with glyceraldehyde-3-phosphate dehydrogenase (GAPDH) and U6 as the internal controls. The relative expression of the genes were calculated using $2^{-\Delta\Delta Ct}$ method. Primer sequences used in this study were shown in Table I.

TUNEL Apoptosis Assay

Tissues embedded in paraffin ahead were sliced to 5 μm-thick sections and subjected to spreading in warm water at 42°C. After baking, paraffin-embedded sections were successfully prepared. Subsequently, paraffin-embedded sections were soaked in xylene solution and graded alcohol for routine deparaffinization until rehydration. TDT solution was added in drops for 1 h of reaction in the dark. Next, deionized water was added dropwise and incubated for 15 min to terminate the reaction. After that, hydrogen peroxide was added in drops to block the activity of endogenous peroxidase, followed by drop-wise addition of working solution for 1 h of reaction. After rinsing, DAB solution was added for color development. Finally, the sections were rinsed again and mounted for observation.

Statistical Analysis

Statistical Product and Service Solutions (SPSS) 20.0 software (IBM Corp., Armonk, NY, USA) was adopted for statistical analysis. The enumeration data were expressed as mean ± stan-

Table I. Primer sequences.

Name	Primer sequence
MiR-204	Forward: 5'TTCCCTTTGTCATCCTATGTGCCT 3'
R	everse: 5'UUCCCUUUGUCAUCCUAUGCCU 3'
Sirt1	Forward: 5'AUGUUAAAUUAUGUAAAGGGAA 3'
	Reverse: 5'CTGGAACCAGTCTGGCCATT 3'
p53	Forward: 5'CTCTCCCACCAACATCCACT 3'
	Reverse: 5'CAACGTCCACCACCATTTGA 3'
U6	Forward: 5' CTCGCTTCGGCAGCACA 3'
	Reverse: 5' AACGCTTCACGAATTTGCGT 3'
GAPDH	Forward primer: 5'ACGGCAAGTTCAACGGCACAG 3'
	Reverse primer: 5'GAAGACGCCAGTAGACTCCACGAC 3'

dard deviation (SD). *t*-test was performed for data meeting normal distribution and homogeneity of variance. Corrected *t*-test was applied for data meeting normal distribution and heterogeneity of variance. Non-parametric test was selected for data not meeting normal distribution and homogeneity of variance. Rank sum test and chi-square test were utilized for ranked data and enumeration data, respectively. $p<0.05$ was considered statistically significant.

Results

Myocardial Morphology Observed via HE Staining

As shown in Figure 1, there was no apparent injury of myocardial tissues in the sham-operation group. Myocardial fibers were arranged orderly, and the cardiomyocyte morphology was normal. Model group exhibited evident injury of myocardial tissues, disorderly arranged and even broken myocardial fibers as well as fragmented and vanished nuclei of cardiomyocytes. In miR-204 mimics group, partial injury was visible in myocardial tissues. Some myocardial fibers were arranged disorderly, and mild damage to cardiomyocytes was observed, which were ameliorated compared with model group.

Positive Expression of Caspase-3 Measured Via Immunofluorescence

According to Figure 2A, there was a low positive expression of Caspase-3 in sham-operation group and a high positive expression of Caspase-3 in the model group. Moreover, the positive expression of Caspase-3 in cardiac tissues increased remarkably in the model group and miR-204 mimics group in comparison with sham-operation group ($p<0.05$). Meanwhile, it was evidently lower in miR-204 mimics group than that in model group ($p<0.05$) (Figure 2B).

Relative Protein Expression Detected Via Western Blotting

There was a binding site between miR-204 and SIRT1, and SIRT1 was the target gene of miR-204 (Figure 3A). The protein expression of SIRT1 was significantly lower in normal group but higher in the model group (Figure 3B). Furthermore, the relative protein expression level of SIRT1 was significantly elevated in the other two groups compared with sham-operation group ($p<0.05$). However, it was markedly lowered in miR-204 mimics group in contrast with model group ($p<0.05$) (Figure 3C).

Results of qRT-PCR

Model group and miR-204 mimics group exerted distinctly lower relative expression of miR-204 but remarkably higher mRNA expressions of SIRT1 and p53 than sham-operation group ($p<0.05$) (Figure 4). However, miR-204 mimics group exhibited prominently higher expression of miR-204 but clearly lower mRNA expressions of SIRT1 and p53 than model group ($p<0.05$).

Apoptosis Rate Detected Via TUNNEL Assay

As shown in Figure 5A, TUNEL-positive cells were sepia. There were fewer TUNEL-positive cells in sham-operation group and more TUNEL-positive cells in model group. The apoptosis rate increased remarkably in model group and miR-204 mimics group when compared with sham-operation group ($p<0.05$). However, it decreased notably in miR-204 mimics group in comparison with that in model group ($p<0.05$) (Figure 5B).

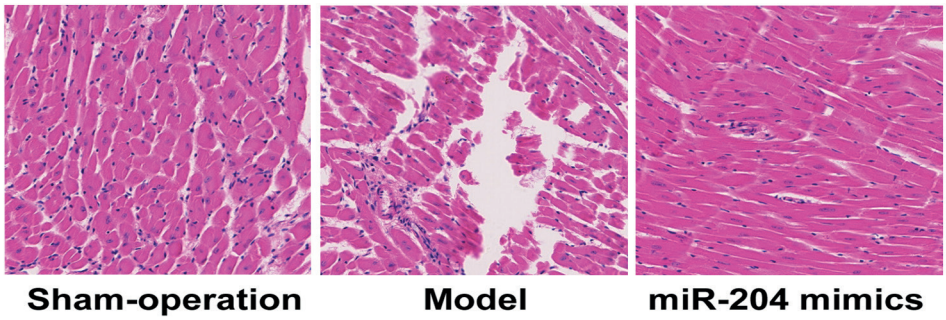

Figure 1. HE staining (magnification: 400×).

Discussion

Ischemic heart disease is a fairly common critical disease in clinic. It usually leads to cardiac dysfunction and even sudden cardiac death due to insufficient myocardial blood supply, seriously endangering people's life and health. Myocardial infarction, a ubiquitous type of ischemic heart disease in clinic, has an increasing morbidity rate year by year. Meanwhile, the affected population is gradually expanded from the elderly to the young[11,12]. Currently, myocardial infarction is becoming more and more harmful. Therefore, deeply studying its pathogenesis, pathological processes and relevant pathological responses is of great significance for searching for efficacious preventive and therapeutic methods and facilitating ventricular remodeling, myocardial repair and

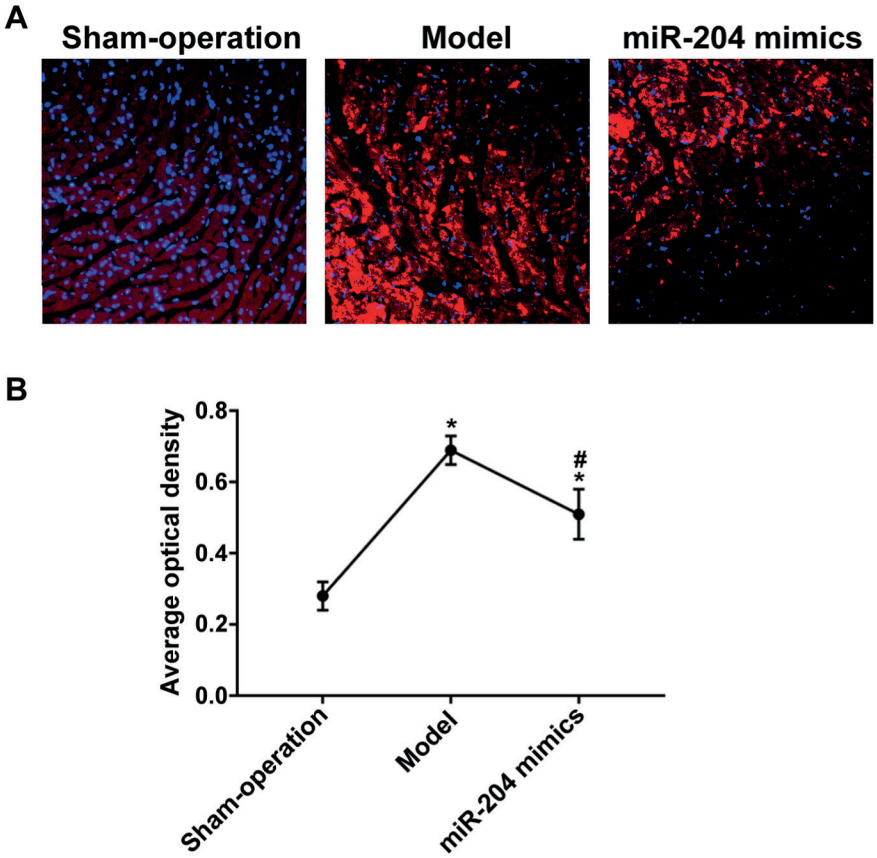

Figure 2. Immunofluorescence results. Note: **A,** Immunofluorescence (magnification: 400×). **B,** Average optical density of positive expression of Caspase-3 in each group. $^{*}p<0.05$ *vs.* sham-operation group, $^{\#}p<0.05$ *vs.* model group.

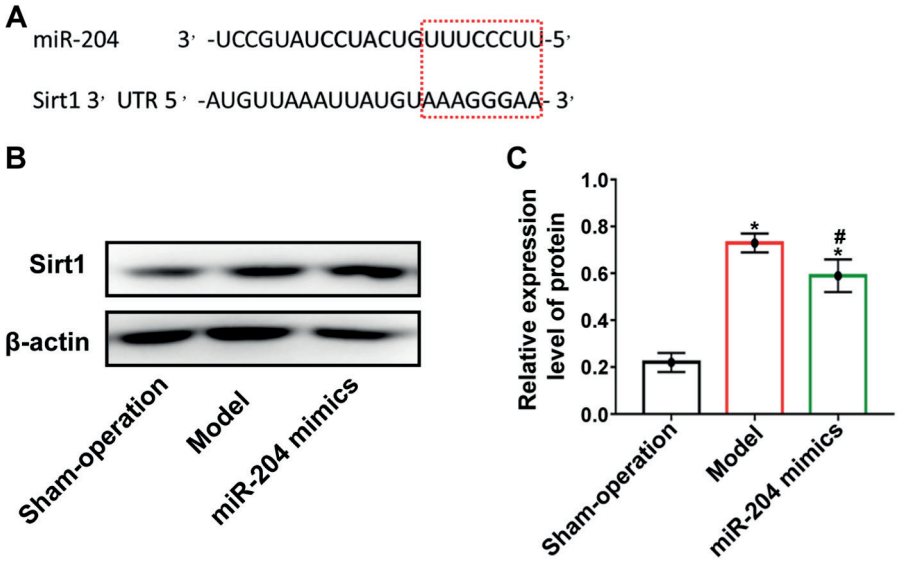

Figure 3. Protein expression detected *via* WB. Note: (**A**) Analysis results of online bioanalysis software, (**B**) WB assay, (**C**) Relative expression level of protein in each group. $^{*}p<0.05$ *vs.* sham-operation group, $^{\#}p<0.05$ *vs.* model group.

functional recovery. The pathological responses after myocardial infarction are very complex, involving massive cardiomyocyte apoptosis and necrosis, fibrosis resulting from excessive proliferation of fibrous tissues, inflammation, etc[13,14]. As the most common physiological and pathological response of cells, apoptosis is activated during the process of myocardial infarction. Following the onset of myocardial infarction, myocardial tissues and cells can produce and release a large amount of apoptosis effector Caspase-3 under hypoxic and ischemic conditions. This may eventually trigger the apoptosis of large quantities of cardiomyocytes[15,16]. In this study, our findings showed that the apoptosis of a large number of cardiomyocytes was observed after myocardial infarction. Meanwhile, the apoptosis effector Caspase-3 was abnormally highly expressed in myocardial tissues. This might be one of the important pathological factors causing massive cardiomyocyte apoptosis after myocardial infarction in the current study.

Upon the incidence of myocardial infarction, the occlusion of feeding arteries of the heart causes ischemia and hypoxia in the initial stage of the disease. In the later stage of myocardial infarction, however, restored blood supply to the feeding arteries of the heart can induce abundant hemoperfusion. After that, ischemia/reperfusion injury occurs. Myocardial ischemia/reperfusion injury is a crucial player in the process of myocardial infarction. It can stimulate the release of numerous inflammation-associated substances, proteins and molecules, so as to aggravate the myocardial tissue injury[17-19]. Meanwhile, myocardial infarction-induced release of inflammatory factors and cytokines is able to activate several

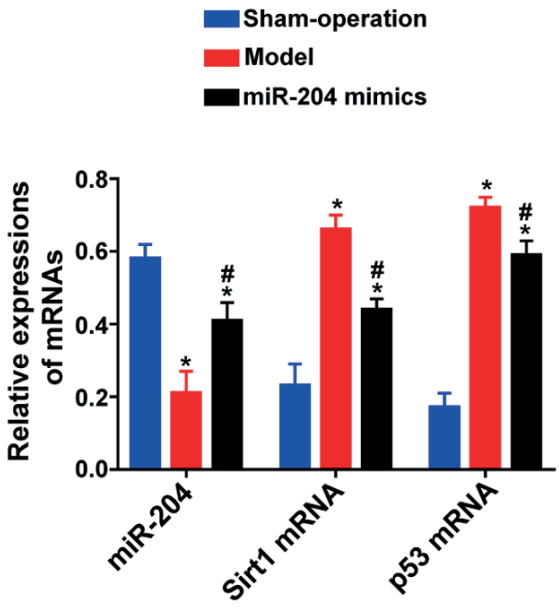

Figure 4. Relative expressions of related mRNAs in each group. Note: $^{*}p<0.05$ *vs.* sham-operation group, $^{\#}p<0.05$ *vs.* model group.

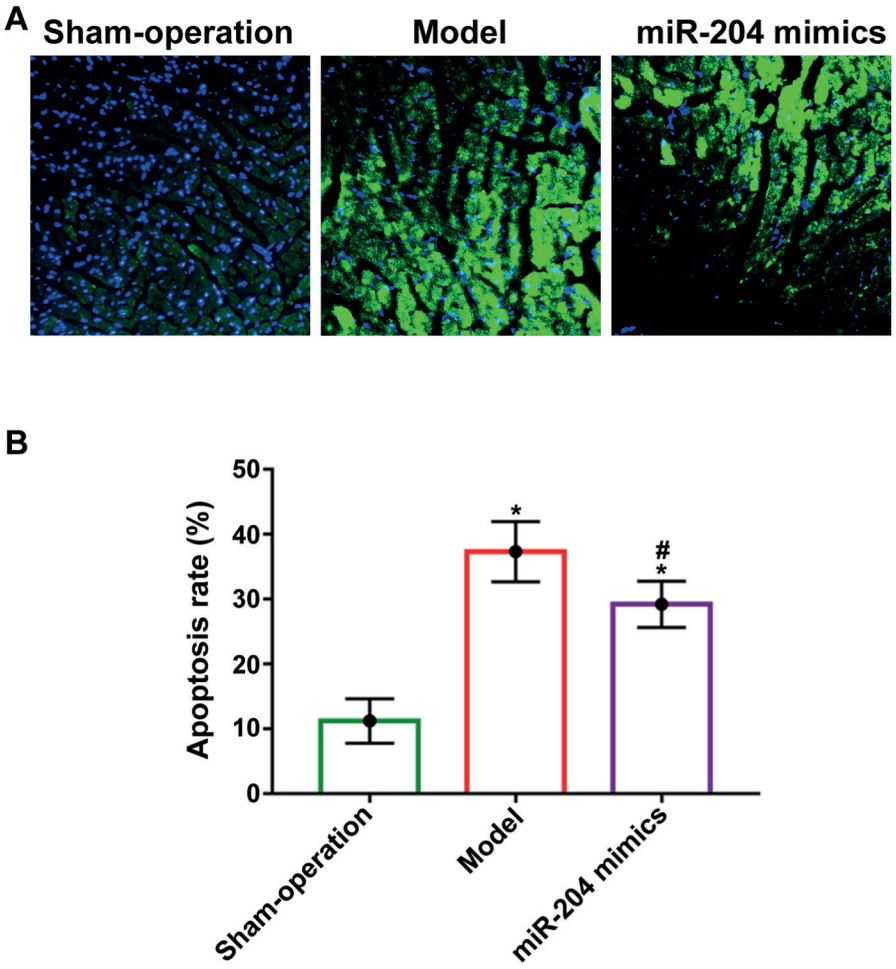

Figure 5. Cell apoptosis detected *via* TUNNEL assay. Note: **A,** TUNNEL assay (magnification: 400×). **B,** Apoptosis rate in each group. $^{*}p<0.05$ *vs.* sham-operation group, $^{\#}p<0.05$ *vs.* model group.

downstream signaling pathways that are definitely correlated with pathological responses, such as inflammation, apoptosis, and necrosis. The SIRT1/p53 signaling pathway is one of the vital signaling pathways in organisms, which has been observed to exert regulatory effects in apoptotic responses. It has been confirmed that SIRT1 inhibits oxidative injury and has anti-inflammatory effects. Meanwhile, SIRT1 is the key molecule of the SIRT1/p53 signaling pathway. In the case of injury, it is highly expressed and can promote the high-level acetylation of downstream p53, thus maintaining the activation of the SIRT1/p53 signaling pathway. Moreover, it plays a pivotal role in regulating cell apoptosis by controlling the expression of downstream Caspase-3, which is closely related to apoptosis. In this research, the protein expression of SIRT1 in cardiac tissues of rats with myocardial infarction was significantly upregulated. The mRNA expressions of SIRT1 and p53 were notably enhanced as well, suggesting that the SIRT1/p53 signaling pathway was prominently activated and functioned in cardiac tissues of rats. Therefore, Caspase-3 served as a downstream effector of the SIRT1/p53 signaling pathway and had an abnormally high expression in cardiac tissues of rats with myocardial infarction as well. All these findings implied that the SIRT1/p53 signaling pathway played crucial roles in the regulation of apoptosis and other pathological processes after myocardial infarction.

MiRNAs are a category of small RNAs possessing vital regulatory effects on a variety of physiological and pathological responses, such as

inflammation, apoptosis, necrosis, and cell proliferation. It has been testified that miR-204[20] is an essential player in the occurrence, development and prognosis of various diseases. It has also become a new hot spot of research due to the regulation of inflammation, apoptosis and other pathological responses. It was verified in this research that miR-204 was aberrantly lowly expressed in cardiac tissues of rats with myocardial infarction. This indicated that miR-204 was inhibited during myocardial infarction, so its normal physiological functions were restrained. Subsequent bioinformatics analysis indicated that SIRT1 was the target gene of miR-204. The inhibitory effect of miR-204 on its target gene SIRT1 was weakened due to its abnormally low expression in cardiac tissues of rats with myocardial infarction. This might eventually lead to the aberrant activation of the SIRT1/p53 signaling pathway. MiR-204 mimics were capable of evidently attenuating the abnormal activation of the SIRT1/p53 signaling pathway and lowering the apoptosis level in cardiac tissues of rats with myocardial infarction. The novelty of this study was that miR-204 reduced the apoptosis level in rats with myocardial infarction *via* targeted inhibition of the SIRT1/p53 signaling pathway.

Conclusions

Shortly, miR-204 can reduce the apoptosis level in rats with myocardial infarction *via* targeted inhibition of the SIRT1/p53 signaling pathway.

Conflict of Interest

The Authors declare that they have no conflict of interests.

References

1) Zhang Z, Guo J. Predictive risk factors of early onset left ventricular aneurysm formation in patients with acute ST-elevation myocardial infarction. Heart Lung 2020; 49: 80-85.
2) Yalta K, Yilmaz MB, Yalta T, Palabiyik O, Taylan G, Zorkun C. Late versus early myocardial remodeling after acute myocardial infarction: a comparative review on mechanistic insights and clinical implications. J Cardiovasc Pharmacol Ther 2020; 25: 15-26.
3) Luo E, Wang D, Qiao Y, Zhu B, Liu B, Hou J, Tang C. Association of total bilirubin with contrast-induced nephropathy in patients with acute ST-elevation myocardial infarction after percutaneous coronary intervention. Coron Artery Dis 2020; 31: 92-94.
4) Xu C, Howey J, Ohorodnyk P, Roth M, Zhang H, Li S. Segmentation and quantification of infarction without contrast agents via spatiotemporal generative adversarial learning. Med Image Anal 2020; 59: 101568.
5) Wu Q, Wang R, Shi Y, Li W, Li M, Chen P, Pan B, Wang Q, Li C, Wang J, Sun G, Sun X, Fu H. Synthesis and biological evaluation of panaxatriol derivatives against myocardial ischemia/reperfusion injury in the rat. Eur J Med Chem 2020; 185: 111729.
6) Gual M, Ariza-Sole A, Formiga F, Carrillo X, Baneras J, Tizon H, Garcia-Picart J, Cardenas M, Regueiro A, Tomas C, Rojas S, Munoz-Camacho JF, Rosas A, Sanchez-Salado JC, Lorente V, Roura G, Alegre O, Gomez-Hospital JA, Lidon RM, Cequier A. Diabetes mellitus is not independently associated with mortality in elderly patients with ST-segment elevation myocardial infarction. Insights from the Codi Infart registry. Coron Artery Dis 2020; 31: 1-6.
7) Zhang Z, Lin J, Nisar M, Chen T, Xu T, Zheng G, Wang C, Jin H, Chen J, Gao W, Tian N, Wang X, Zhang X. The Sirt1/P53 axis in diabetic intervertebral disc degeneration pathogenesis and therapeutics. Oxid Med Cell Longev 2019; 2019: 7959573.
8) Lin XL, Li K, Yang Z, Chen B, Zhang T. Dulcitol suppresses proliferation and migration of hepatocellular carcinoma via regulating SIRT1/p53 pathway. Phytomedicine 2020; 66: 153112.
9) Yuan H, Zhang J, Li F, Li W, Wang H. Sinomenine exerts antitumour effect in gastric cancer cells via enhancement of miR-204 expression. Basic Clin Pharmacol Toxicol 2019; 125: 450-459.
10) Xu G, Thielen LA, Chen J, Grayson TB, Grimes T, Bridges SJ, Tse HM, Smith B, Patel R, Li P, Evans-Molina C, Ovalle F, Shalev A. Serum miR-204 is an early biomarker of type 1 diabetes-associated pancreatic beta-cell loss. Am J Physiol Endocrinol Metab 2019; 317: E723-E730.
11) Sanri US, Ozsin KK, Toktas F, Yavuz S. Appropriate surgical repair of ventricular free wall rupture after infarction: a case report. Braz J Cardiovasc Surg 2020; 34: 775-778.
12) Edqvist J, Rawshani A, Adiels M, Bjorck L, Lind M, Svensson AM, Gudbjornsdottir S, Sattar N, Rosengren A. Contrasting associations of body mass index and hemoglobin a1c on the excess risk of acute myocardial infarction and heart failure in type 2 diabetes mellitus. J Am Heart Assoc 2019; 8: e13871.
13) Zhao Z, Du S, Shen S, Wang L. MicroRNA-132 inhibits cardiomyocyte apoptosis and myocardial remodeling in myocardial infarction by targeting IL-1beta. J Cell Physiol 2020; 235: 2710-2721.
14) Zalghout S, Kaplan A, Abidi E, El-Achkar GA, Nour-Eldine W, Khalil AA, Kobeissy F, Husari A, Habib A, Zouein FA, Hamade E. Tobacco cigarette smoking exacerbates aortic calcification in an early stage of myocardial infarction in a female mouse model. J Cell Physiol 2020; 235: 1568-1575.

15) Mitra A, Ray A, Datta R, Sengupta S, Sarkar S. Cardioprotective role of P38 MAPK during myocardial infarction via parallel activation of alpha-crystallin B and Nrf2. J Cell Physiol 2014; 229: 1272-1282.

16) Fan YZ, Huang H, Wang S, Tan GJ, Zhang QZ. Effect of lncRNA MALAT1 on rats with myocardial infarction through regulating ERK/MAPK signaling pathway. Eur Rev Med Pharmacol Sci 2019; 23: 9041-9049.

17) Silva-Palacios A, Ostolga-Chavarria M, Sanchez-Garibay C, Rojas-Morales P, Galvan-Arzate S, Buelna-Chontal M, Pavon N, Pedraza-Chaverri J, Konigsberg M, Zazueta C. Sulforaphane protects from myocardial ischemia-reperfusion damage through the balanced activation of Nrf2/AhR. Free Radic Biol Med 2019; 143: 331-340.

18) Li L, Li X, Zhang Z, Liu L, Liu T, Li S, Liu S, Zhou Y, Liu F. Effects of hydrogen-rich water on the pi3k/akt signaling pathway in rats with myocardial ischemia-reperfusion injury. Curr Mol Med 2019: (DOI: 10.2174/1566524019666191105150709).

19) Chen M, Li X, Yang H, Tang J, Zhou S. Hype or hope: Vagus nerve stimulation against acute myocardial ischemia-reperfusion injury. Trends Cardiovasc Med 2019: (DOI: 10.1016/j.tcm.2019.10.011).

20) Zhang Z, Wang W, Liu JB, Wang Y, Hao JD, Huang YJ, Gao Y, Jiang H, Yuan B, Zhang JB. Ssc-miR-204 regulates porcine preadipocyte differentiation and apoptosis by targeting TGFBR1 and TGFBR2. J Cell Biochem 2020; 121: 609-620.